

ZIF-8/styrene-IL polymerization hollow fiber membrane for improved CO₂/N₂ separation

Wen-Hsiung Lai^a, David K. Wang^b, Ming-Yen Wey^{a,*}, Hui-Hsin Tseng^{a,**}

^a Department of Environmental Engineering, National Chung Hsing University, Taichung, 402, Taiwan, ROC

^b School of Chemical and Biomolecular Engineering, The University of Sydney, Sydney, Australia

ARTICLE INFO

Handling Editor: Zhen Leng

Keywords:

Hollow fiber
Mixed matrix membrane
ZIF-8
Ionic liquid
CO₂ separation

ABSTRACT

Compared to supported ionic liquid membranes, poly(ionic liquid) membranes are synthesized by the polymerization of ionic liquid monomers to develop polymeric backbone to improve its membrane stability for gas separation process. However, the resulting dense membrane structure induced the lower gas permeance of the poly(ionic liquid) membranes. To overcome this limitation, in this study, ZIF-8, possessing the property of molecular sieves, was added to poly(styrene-ionic liquid) hollow fiber membranes (p(SIL) HFMs), providing a transport pathway. SIL monomers with different lengths of alkyl chain were polymerized and integrated with ZIF-8 fillers to synthesize ZIF-8/poly(ionic liquid) mixed matrix hollow fiber membranes (ZIF-8/p(SIL) MMHFMs). When the chain length of SIL monomers was increased, the CO₂ permeance of p(SIL) HFMs increased from 3.6 to 4.6 GPU, while CO₂/N₂ selectivity decreased from 29 to 23. Additionally, the CO₂ permeance of ZIF-8/p(SIL) MMHFMs was enhanced by 33% compared to that of p(SIL) HFMs. However, chain rigidification phenomenon was observed which cause the ZIF-8/p(SIL) MMHFMs showed the decreasing CO₂ permeance when the ZIF-8 content was increased. The best separation performance of ZIF-8/p(SIL) MMHFMs was obtained with 0.5 wt% ZIF-8 addition, which exhibited a CO₂ permeance and CO₂/N₂ selectivity of 6 GPU and 30. Therefore, adding ZIF-8 into p(SIL) HFMs to form the ZIF-8/p(SIL) MMHFMs is beneficial to enhance the CO₂ permeance of membranes because of the characteristic of the pore size of 3.4 Å and transport pathway provided by ZIF-8 fillers.

1. Introduction

Ionic liquids (ILs), comprising cations and anions, are regarded as potential materials for CO₂ capture due to the high CO₂ affinity (Sasikumar et al., 2018), which was induced by the Lewis acid–base interaction between the anion structure of the CO₂ gas molecules (Lewis base) and ILs (Lewis acid) (Ghasemi Estahbanati et al., 2017; Shamair et al., 2020). Additionally, ILs exhibit high thermal stability and a low vapor pressure. Therefore, the issue of material loss through evaporation during gas separation can be overcome by replacing organic solvents with ILs (Liang et al., 2014).

Supported ionic liquid membranes (SILMs) are common configurations derived from ILs for gas separation processes. SILMs were prepared using porous substrates immersed in an IL solution. The ILs coated the external surface of the porous substrates via capillarity forces (Ceratti et al., 2015; Lai et al., 2020). In addition, lower IL amounts were used to effectively reduce the cost of membrane synthesis (Lai et al., 2022).

However, the stability and operability of SILMs for application in gas separation processes is a challenge. Moreover, a “blowout” phenomenon caused by the extrusion of the ILs from the substrates was observed when the SILMs were operated at high transmembrane pressures (Kammakam et al., 2020; Tomé et al., 2014). The effects of certain parameters, such as the pore size of the substrate (Lai et al., 2020), viscosity of the ILs (Neves et al., 2010) and hydrophilicity between the ILs and substrates (Neves et al., 2010; Ríos et al., 2007), on the stability of SILMs were discussed.

For improving the operability of IL-derived membranes, poly(IL) membranes were polymerized from the IL monomers. Therefore, the polymeric backbone is produced from the repeated polymerized IL monomers (Li et al., 2021). Styrene, which features a vinyl functional group that combines with IL monomers, is an ideal precursor to synthesize IL polymers (Friess et al., 2021). Compared to SILMs, poly(IL) membranes exhibit a higher membrane stability for gas separation. Tang et al. mentioned that imidazolium-derived polymeric ionic liquids (PILs)

* Corresponding author. National Chung Hsing University, Department of Environmental Engineering, 145, Xingda Rd., Taichung, 402, Taiwan, ROC

** Corresponding author. National Chung Hsing University, Department of Environmental Engineering, 145, Xingda Rd., Taichung, 402, Taiwan, ROC.

E-mail addresses: mywey@dragon.nchu.edu.tw (M.-Y. Wey), hhtseng@nchu.edu.tw (H.-H. Tseng).

showed higher CO₂ absorption capacities than the corresponding ILs (Tang et al., 2008). However, the poly(IL) membranes exhibit lower gas permeability and diffusivity in the gas separation process. It is a challenge that should be addressed (Tomé and Marrucho, 2016). This substantial cause the poly(IL) membranes to form the dense membrane structure and show the lower gas permeability and diffusivity. Therefore, it caused the increasing gas transmission resistance (Bara et al., 2008b, 2009). Moreover, because of the high brittleness of the poly(IL) membranes, their mechanical strength is of significant concern (Bara et al., 2007).

Mixed matrix membranes (MMMs), synthesized from the polymeric matrix and inorganic particles, integrates the advantages of polymers and inorganic materials with the characteristic of economical processability and high gas separation performance, respectively (Huang et al., 2020; Lin et al., 2022). Therefore, MMMs are considered as an attractive membrane configuration to overcome the trade-off of membrane in current gas separation technologies. Additionally, the mechanical strength of MMMs was enhanced when fillers were integrate with the polymer phase (Aroon et al., 2010; Ismail et al., 2009; Lin et al., 2021).

Zeolitic imidazolate framework-8 (ZIF-8), a subclass of metal organic frameworks, consists of 2-methylimidazole and transition metal ions (Zn²⁺ or Co²⁺) exhibits unique molecular sieve properties and structural tenability (Lin et al., 2021; Yuan et al., 2022). Because of the specific pore size of 3.4 Å in the ZIF-8 frameworks, ZIF-8 has been widely applied in H₂/CH₄ (Wijanayake et al., 2013, 2014), CO₂/CH₄ and CO₂/N₂ (Dai et al., 2012) separation processes (Basu et al., 2011; Guan et al., 2020; Nik et al., 2012; Wang et al., 2020). The organic-inorganic properties of ZIF-8 is beneficial to improve the compatibility between ZIF-8 particles and polymer in MMMs and reduce the formation of defect (Perez et al., 2009; Wijanayake et al., 2013). The effects of loading and morphology on the performance of the ZIF-8 derived MMMs were investigated in previous studies (Lai et al., 2019, 2021; Zhuang et al., 2018). The particle size and morphology of ZIF-8 are influential factors that influence the separation performance of MMMs. Compared to the MMMs prepared using cubic ZIF-8, the formation of defects was decreased at the interface between the ZIF-8 particles and the polymer matrix because the disruption of the polymer chains was avoided when MMMs were synthesized by the ZIF-8 which showed the blunt outer morphology. Meanwhile, the smaller particle size of ZIF-8 provides a larger polymer-filler interface, which is beneficial for improving the compatibility of ZIF-8 and the polymer (Nordin et al., 2014). Additionally, the π - π interaction induced by the aromatic rings of the polymer chain and 1-hexyl-3-methyl-imidazolium (Hmim) enhanced the adhesion of ZIF-8 to the polymer matrix (Lai et al., 2021; Wang et al., 2017). Therefore, compared to the pure polymer membranes, the H₂ permeance of the MMMs increased from 0.87 to 1.8 GPU (2.06 folds) when MMMs were prepared using 50 wt% ZIF-8.

In our previous study, the stability of ionic liquid hollow fiber membranes (SILHFMs) can be improved by controlling the outer surface morphology of hollow fiber substrates. However, ionic liquids still squeezed from the pore of hollow fiber substrates when the SILHFMs were operated at the transmembrane pressure over 2.5 bar (Lai et al., 2020). In order to improve the operability of ionic liquid membrane, we prepared the polymerized styrene-ionic liquid hollow fiber membranes (p(SIL) HFMs) by preparing the polymeric backbone between the S-IL monomers during polymerization process. However, compared the HFSILMs, the CO₂ permeance of p(SIL) HFMs decreased by 50% due to the dense membrane structure of HFSILMs (Lai et al., 2022). Therefore, in this study, we integrate the ZIF-8 nanoparticles into p(SIL) HFMs to prepare the ZIF-8/p(SIL) mixed matrix hollow fiber membranes (ZIF-8/p(SIL) MMHFMs) for enhancing the CO₂ permeance of membranes. Polymerized styrene-ionic liquid hollow fiber membranes (p(SIL) HFMs) are potential membranes for CO₂ separation. Dense polymer backbones were synthesized using polymerized IL monomers to form a dense membrane structure for improving the membrane stability in high transmembrane pressure. However, their application in gas separation

processes has been limited owing to the low gas permeance of dense structure. ZIF-8 nanoparticles, which exhibited the characteristic of the pore size of 3.4 Å and transport pathway, were selected as an ideal filler to beneficially enhance the diffusion of CO₂ gas molecules. Additionally, Hollow fibers were considered as an attractive configuration for gas separation systems, because they exhibited favorable advantages, such as self-support, large surface area per unit volume and easy processing (Ma et al., 2015; Peng and Chung, 2008). Additionally, hollow fiber can be used to prepare the SILHFMs by dip-coating methods which is beneficial to reduce the quantities of ILs to prepare the thin but selective IL layers on the outer surface of hollow fiber. Therefore, it can decrease the cost of membrane preparation and form the SILHFMs with high CO₂ separation performance. Additionally, we has investigated the effect of the substrate morphology and IL coating behavior on the gas separation performance of SILHFMs (Lai et al., 2020). Further, the polymerization parameters (e.g., the precursor concentration and UV duration) for supported p(SIL) HFMs was discussed to optimize the on the separation performances of supported p(SIL) HFMs (Lai et al., 2022). In this study, we incorporated the ZIF-8 nanoparticles in the p(SIL) HFMs to form the mixed matrix membrane structure for enhancing the gas permeance of membranes. Therefore, the compatibility between different alkyl length of styrene-ionic liquids and ZIF-8 was discussed. Further, the effect of ZIF-8 loading on the gas separation performance of ZIF-8/p(SIL) MMHFMs was investigated.

2. Experimental

2.1. Materials

The chemicals 1-methylimidazole (Cas No. 616-47-7) and 1-ethylimidazole (Cas No. 1072-62-4) were purchased from Alfa Aesar, and 1-(n-Butyl)imidazole (Cas No. 4316-42-1) was obtained from Matrix Scientific. Zinc nitrate hexahydrate (98%), 2-hydroxy-2-methylpropionophenone (Cas No. 7473-98-5), and 4-chloromethylstyrene (Cas No. 1592-20-7) were obtained from Sigma-Aldrich. Ammonium hydroxide (28%), and toluene were purchased from Union Chemical Works Ltd. *N*-methyl-2-pyrrolidinone (NMP) and ethyl acetate (EtOAc, Cas No. 141-78-6) were purchased from Macron Fine Chemicals., Diethyl ether (Et₂O, Cas No. 60-29-7) was obtained from Honeywell and acetonitrile (Cas No. 75-05-8) was purchased from J. T. Baker. Bis(trifluoromethane) sulfonimide lithium (LiTf₂N, Cas No. 90076-65-6) was obtained from TCI America. The waste plastic containers prepared by SBC polymer were used as the membrane material to synthesize wSBC-HF substrates (Lai et al., 2020).

2.2. wSBC-HF substrate fabrication

First, 17.13 g wSBC was dissolved in the 50 mL NMP solvent to prepare the dope solution. The flow rate was controlled by the syringe pumps (Isco, Model 500D, Lincoln, NE) to extrude the bore solution (DI water) (10 mL/min) and the polymeric dope solution (20 mL/min). The nascent hollow fibers were extruded into a water coagulation bath with the air gap distance of 0 cm. The hollow fiber substrates were immersed in methanol and tap water for 3 times, respectively (Albo et al., 2014), and dried in an oven at 80 °C for 24 h to remove the solvent.

2.3. ZIF-8 synthesis

The synthesis of ZIF-8 particles using 2.97 g of Zn(NO₃)₂ and 1.64 g of Hmim dissolved in 29 and 20 mL of NH₄(OH) solutions, respectively, and were stirred for 1 h. Thereafter, the Zn(NO₃)₂ solution was rapidly mixed with the Hmim solution and stirred for 5 h at 30 °C to synthesize ZIF-8 particles. Subsequently, the ZIF-8 particles were washed with MeOH until the pH of the solution was 7 and separated by centrifugation. Finally, the ZIF-8 particles were dried in an oven at 80 °C for 12 h for solvent removal.

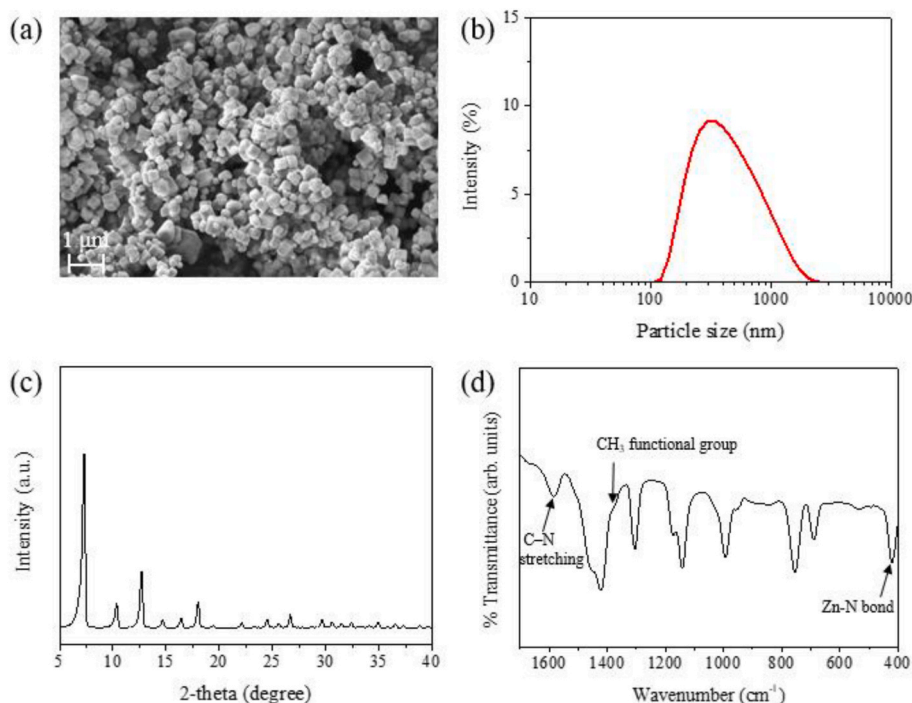


Fig. 1. (a) SEM images, (b) particle size distribution, (c) XRD pattern, and (d) FTIR spectrum of ZIF-8 (Lai et al., 2021).

2.4. Synthesis of SIL monomers

SIL monomers were synthesized using cations with alkyl side chains of different lengths according to a procedure described in literature (Bara et al., 2007). First, the molar ratio of imidazole and 4-chloromethylstyrene precursors were controlled at 1:1 and dissolved in 30 mL CH_3CN at the controlled temperature of 50°C and stirring for 12 h. 250 mL Et_2O was poured into the intermediate solution and stored in a 4°C for 6 h. Subsequently, the precipitated solutions were obtained after freezing. The Et_2O solvent was poured out of the bottle, and DI water (125 mL) was used to dissolve the ionic product. Then, 100 mL EtOAc was used to wash ionic product/DI water mixed solution for three times. 8.79 g LiTf_2N was added to the ionic product/DI water mixed solution with stirring for 1 h, which immediately produced the product like oily liquid. The oily liquid was extracted with EtOAc (250 mL) and washed three times with DI water (100 mL). Subsequently, the final materials were dried over anhydrous MgSO_4 for water removal, and rotatory evaporation was used to remove the EtOAc solution from the SIL product. The SIL monomers were denoted as $y\text{C}$, where y is the length of the alkyl chain. ^1H NMR of 1C (DMSO, 550 MHz): 9.19 (s, N-CH-N), 7.78 (s, N-CH=CH-N), 7.71 (d, Ph), 7.75 (d, Ph), 6.75 (m, CH=CH₂), 5.89, 5.31 (d, CH=CH₂), 5.40 (s, Ph-CH₂-N), and 1.17 ppm (t, N-CH₃) (Lai et al., 2022). ^1H NMR of 2C (DMSO, 550 MHz): 9.28 (s, N-CH-N), 7.81 (s, N-CH=CH-N), 7.53 (d, Ph), 7.40 (d, Ph), 6.73 (m, CH=CH₂), 5.89, 5.31 (d, d, CH=CH₂), 5.42 (s, Ph-CH₂-N), 4.2 (t, N-CH₂-CH₃), and 1.17 (t, N-CH₂-CH₃). ^1H NMR of 4C (DMSO, 550 MHz): 9.29 (s, N-CH-N), 7.80 (s, N-CH=CH-N), 7.53 (d, Ph), 7.40 (d, Ph), 6.73 (m, CH=CH₂), 5.89, 5.31 (d, d, CH=CH₂), 5.42 (s, Ph-CH₂-N), 4.2 (t, N-CH₂-CH₂-CH₂-CH₃), 1.79 (m, N-CH₂-CH₂-CH₂-CH₃), 1.26 (m, N-CH₂-CH₂-CH₂-CH₃), and 0.90 (t, N-CH₂-CH₂-CH₂-CH₃).

2.5. Preparation of ZIF-8/p(SIL) MMHFMs

The preparation of ZIF-8/p(SIL) MMHFMs were carried out by the dip-coating method. First, the ZIF-8 particles were added to the SIL solution to prepare the ZIF-8/SIL coating solution. The bottom of wSBC hollow fiber substrates were sealed by the epoxy. The 120 mm/min

immersion rate was controlled to immerse substrates into the ZIF-8/SIL coating solution and stay for 10 s. Subsequently, the 365 UV lamp was used to polymerize the intermediate membranes with the controlled intensity of 8.5 mW/cm^2 for 30 min to form ZIF-8/p(SIL) MMHFMs. To denote the ZIF-8/p(SIL) MMHFMs, the formula $x\text{Z-p}(y\text{C})$ was used, where x is the weight of ZIF-8 addition in the ZIF-8/SIL coating solution, and y is the alkyl side chain of the SIL monomers. Pure p(SIL) HFMs were synthesized from the SIL monomers without the addition of ZIF-8. The prepared p(SIL) HFMs were denoted as p($y\text{C}$).

2.6. Single gas permeation tests

The single gas separation performance of the ZIF-8/p(SIL) MMHFMs was determined using the constant-volume/variable-pressure method. Three identical samples were tested three times each, and the average values were reported. First, the ZIF-8/p(SIL) MMHFMs were sealed with an epoxy resin in a membrane cell and degassed for 1 h by a vacuum pump. The 3 bar transmembrane pressure (p_0) was controlled at upstream system for the experiments, and the computer was used to record the change of pressure in the downstream. The straight line in the steady state region was used to calculate the slope (dp/dt (cmHg/s)). The permeance (P) and selectivity (α) of membranes were estimated by the equations as following:

$$\text{Permeance (GPU)} = P = 10^6 \times \frac{273.15 \times V}{76A \times T \times p_0} \times \frac{dp}{dt} \quad (1)$$

$$\alpha_{i/j} = \frac{P_i}{P_j} \quad (2)$$

where P is the membrane permeance with the unit of GPU [$\text{GPU} = 1 \times 10^{-6} \text{ cm}^3 \text{ (STP)/cm}^2 \text{ s cm Hg}$], dp/dt is the pressure change of the downstream chamber in the steady state region (cm-Hg/s); V is the downstream volume (cm^3); T is the operating temperature (K); A is the effective membrane area (cm^2); p_0 is the operating pressure in the upstream region (cm-Hg), and $\alpha_{i/j}$ is the gas selectivity of gas molecule i over gas molecule j .

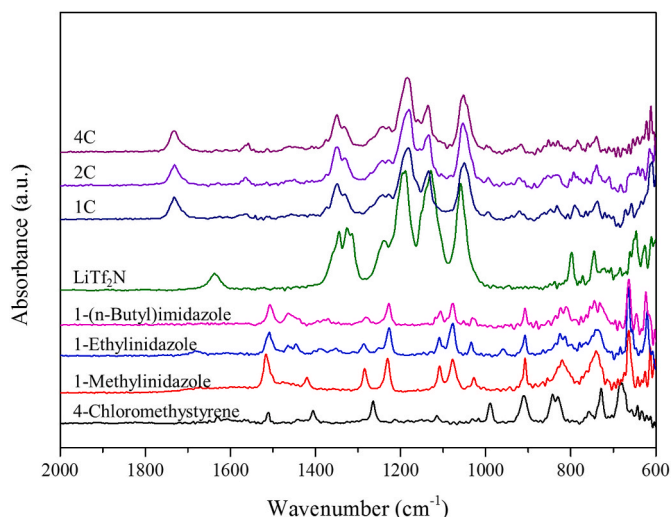


Fig. 2. FTIR analysis of SIL series monomers and precursors (Lai et al., 2022).

3. Results and discussion

3.1. Characteristic of ZIF-8

The ZIF-8 was characterized using FE-SEM (Fig. 1 (a)). Compared to the ZIF-8 synthesized using a water solution, the morphology of ZIF-8 was blunt and showed a smaller particle size of 120 nm (Fig. 1(b)). The blunt ZIF-8 was induced by the Hofmeister anion effect, which was occurred between the anions in the precursor solution (Chen et al., 2014b). This is because the synthesis of ZIF-8 is effectuated via Hmim deprotonation. When the ammonia solution content was increased, excess protons were produced because of the fast deprotonation of Hmim. Therefore, the ZIF-8 outer morphology was transformed from rhombic shape to blunt shape. The synthesis of ZIF-8 particles included Hmim deprotonation and bridging with Zn^{2+} ions. Hmim decompose to H^+ and mim^- during the process of Hmim deprotonation. Then, Zn^{2+} ions react with the mim^- to form a nucleation unit of ZIF-8. Furthermore, Hmim is the basic ligands with the $pK_a = 14.2$ (Kimura et al., 1991). Jian et al. (2015) reported that the deprotonation of Hmim was not easily occurred in aqueous solution due to its low K_a value.

Therefore, the deprotonation of Hmim could be driven by increasing the basicity of solution (He et al., 2014). The nucleation rate increased with the increasing amount of the basic solution used and resulted in a reduction of the ZIF-8 particle size (Chen et al., 2014a; Cravillon et al., 2011). The X-ray diffraction (XRD) pattern of ZIF-8 is shown in Fig. 1(c). The peaks at $2\theta = 7.30^\circ, 10.35^\circ, 12.70^\circ, 14.80^\circ, 16.40^\circ,$ and 18.00° correspond to (110), (200), (211), (220), (310), and (222) planes, respectively, which are consistent with observations of previous studies (He et al., 2014; Kida et al., 2013). Therefore, the structure of ZIF-8 was assigned as the SOD-type. Fig. 1(d) shows the spectrum of Fourier-transform infrared (FTIR), which showed the functional groups of ZIF-8. ZIF-8 was built from the tetrahedral transition metal, Zn^{2+} , and bridged by the Hmim ligands. Therefore, the peak of the Zn–N bond was observed at 422 cm^{-1} . Moreover, the peaks observed at 1384 and 1580 cm^{-1} corresponding to the $-CH_3$ groups and C–N stretching vibration in the structure of Hmim, respectively (Lai et al., 2019; Ordoñez et al., 2010).

3.2. FTIR and NMR characterization of SIL monomers

The precursors and SIL monomers were characterized using the ATR–FTIR spectra (Fig. 2). The C–N–C and C=N vibrations peaks were observed at 1076 and 1500 cm^{-1} , which was corresponding to 1-methylimidazole, 1-ethylimidazole, and 1-(n-butyl)imidazole. In the analysis result of 4-chloromethyl styrene, the C–Cl functional group peak was observed at 675 cm^{-1} (Chen et al., 2013).

The absorption peaks at $1357, 1064, 1250\text{--}1150, 1140,$ and 1064 cm^{-1} represent the vibrations of S–N–S and SO_2 stretching, which were derived from the Tf_2N^- anion.

In the 1C, 2C, and 4C spectra, the characteristic peaks at 675 (C–Cl) and 1500 cm^{-1} (C=N) were insignificant, indicating the successful formation of the intermediate products from the 4-chloromethyl styrene and imidazole precursors. All characteristic peaks of the Tf_2N^- anions were observed in the 1C, 2C, and 4C spectra.

Furthermore, 1H NMR spectroscopy was used to analyze the cation chemical structures of 1C, 2C, and 4C (Fig. S1). Ph– CH_2 –N in the SIL cation was observed at 5.40 ppm . This indicates that the 4-chloromethyl styrene and imidazole precursors were successful in synthesizing the SIL cation. The full 1H NMR data for SIL are presented in Section 2.3.

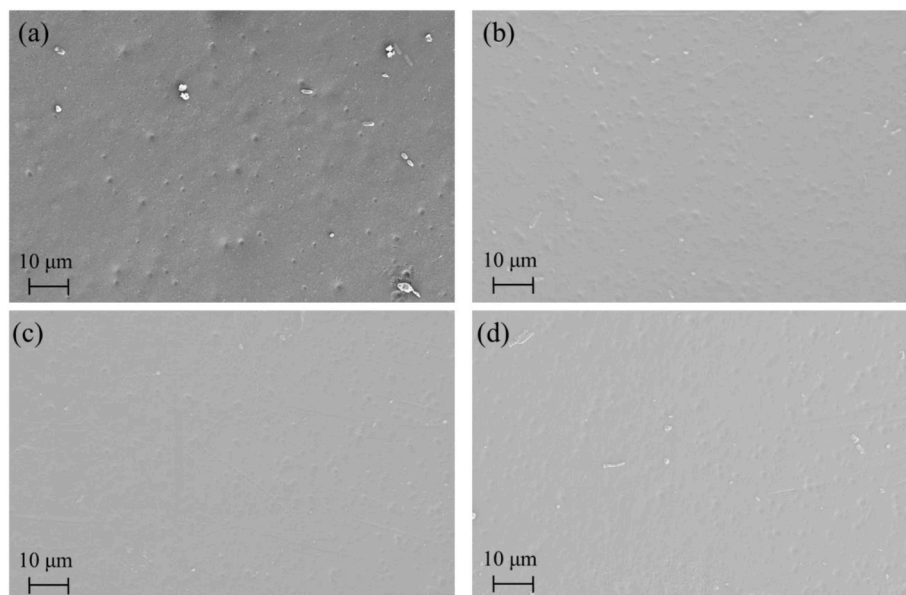


Fig. 3. Outer surface of (a) wSBC substrate, (b) p(1C), (c) p(2C), and (d) p(4C).

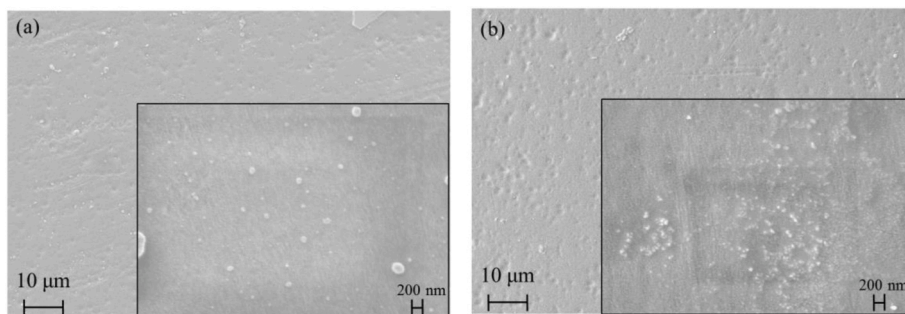


Fig. 4. Outer surface of (a) 1Z-p(1C) and (b) 5Z-p(1C).

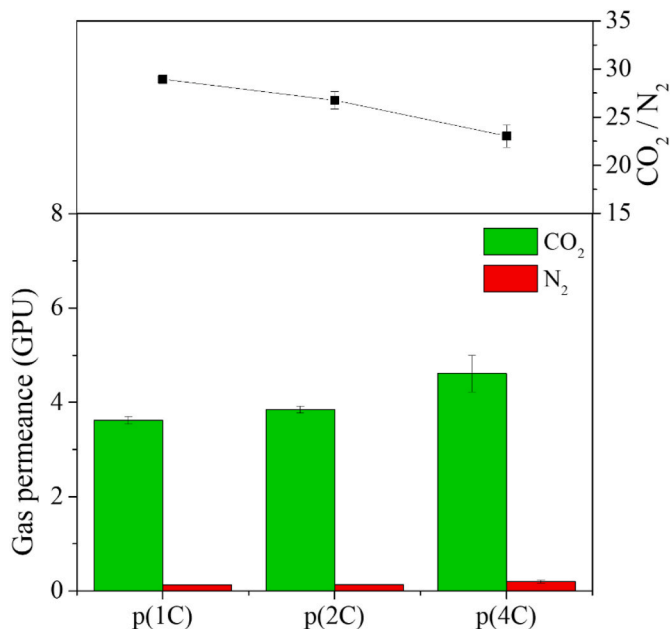


Fig. 5. Gas separation performance of p(SIL) HFMs with different alkyl chain lengths.

3.3. Outer surface of p(SIL) series membranes

The outer surfaces of the substrates and membranes were characterized using FE-SEM, as shown in Fig. 3. Small pores were observed on the outer surface of the wSBC-HF substrate (Fig. 3(a)). These pores were induced by the fast phase inversion when the nascent wSBC-HF extruded into the coagulation bath. When the hollow fibers were immediately immersed into the coagulation bath with 0 cm air gap (Hosseini et al., 2010), it caused the rapid solvent exchange and water diffusion

occurred, resulting in rapid phase separation on the outer surface of the hollow fiber substrate (Chung and Hu, 1997). Therefore, the small pores were induced by chain contraction. Compared to the wSBC-HF substrates, the outer surface of the p(SIL) HFMs became smooth when the SIL monomers were polymerized (Fig. 3(b–d)). This illustrated that the SIL monomers featured ideal compatibility to adhere to the wSBC-HF substrates. Therefore, the selective p(SIL) layer synthesized using the SIL monomers was efficient in smoothing and modifying the outer surface of the wSBC-HF substrates.

The dispersion of ZIF-8 on the surface of the ZIF-8/p(SIL) MMHFMs (p(1C)- series) is shown in Fig. 4. The exterior of the ZIF-8/p(SIL) MMHFMs exhibited a smooth surface when SEM images were observed at a magnification of 1000x. When the magnification was increased from 1000x to 20,000x, ZIF-8 aggregation was observed with the increasing content of ZIF-8. ZIF-8 was well distributed when a 1 wt% ZIF-8 was added. However, the agglomeration of ZIF-8 was observed on the outer surface of 5Z-p(1C). In addition, effects of the addition and agglomeration of ZIF-8 on the separation performance of the ZIF-8/p(SIL) MMHFMs were investigated in Section 3.4.

3.4. Separation performance of ZIF-8/p(SIL) MMHFMs

3.4.1. Effect of the alkyl chain length

Fig. 5 shows the separation performance of p(SIL) HFMs prepared using SIL monomers with different alkyl chain lengths. The CO₂ permeance of the p(SIL) HFMs increased from 3.6 to 4.6 GPU when the alkyl chain length of the SIL monomers was increased from C₁ to C₄. However, the CO₂/N₂ selectivity of the p(SIL) HFMs exhibited a trend opposite to that of the CO₂ permeance. In addition, the CO₂/N₂ selectivity of the p(SIL) HFMs decreased from 29 to 23 when the alkyl chain length was increased. An increase in the alkyl chain length of the cation led to an increase in the CO₂ and N₂ permeance of the p(SIL) HFMs but resulted in a decrease in the ideal CO₂/N₂ selectivity. It was speculated that the inefficient packing of the alkyl side chains was induced by the increase in the alkyl chain length on the cation of the SIL monomers (Bara et al., 2007; Cowan et al., 2016). Therefore, a free volume was formed in the p

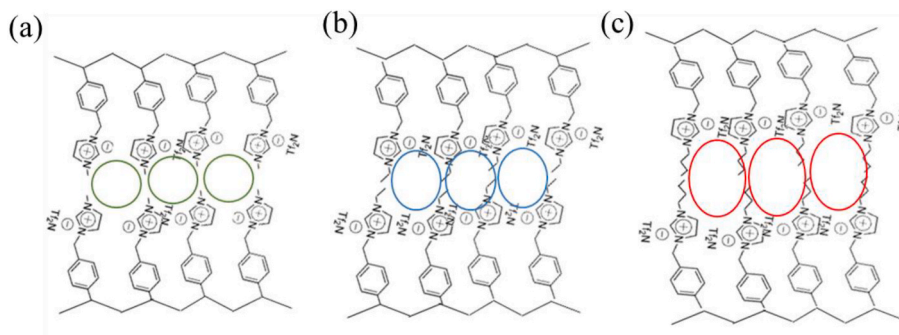
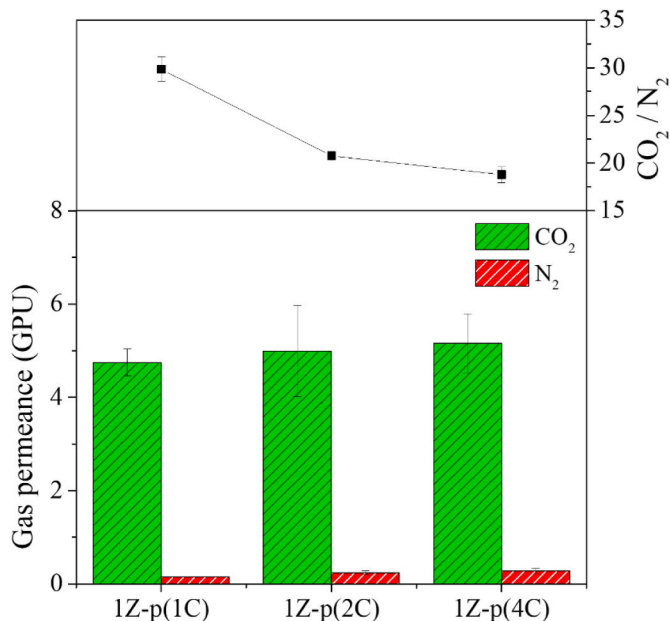


Fig. 6. Schematic of the chain packing of (a) p(1C), (b) p(2C), and (c) p(4C).

Table 1CO₂ and N₂ diffusivity (*D*) and solubility (*S*) of p(SIL) HFMs.

Name	D_{CO_2} ($\times 10^{-8}$ cm ² /s)	S_{CO_2} ($\times 10^{-2}$ cm ³ (STP)/cm ³ cm-Hg)	D_{N_2} ($\times 10^{-8}$ cm ² /s)	S_{N_2} ($\times 10^{-2}$ cm ³ (STP)/cm ³ cm-Hg)	D_{CO_2}/D_{N_2}	S_{CO_2}/S_{N_2}
p(1C)	18.6	9.8	6.9	0.9	2.7	10.4
p(2C)	33.9	5.7	7.2	1.0	4.7	5.8
p(4C)	92.8	2.5	8.3	1.2	11.1	2.1

**Fig. 7.** Gas separation performance of ZIF-8/p(SIL) MMHFMs with different alkyl chain lengths.

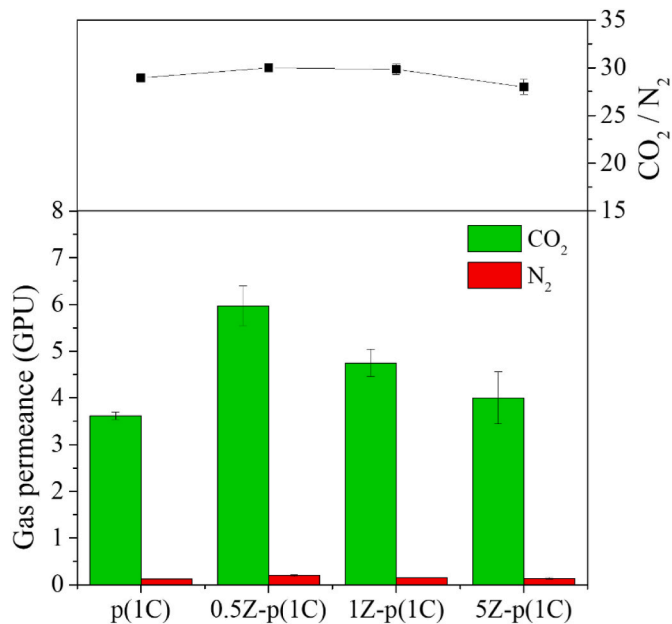
(SIL) HFMs, which caused a lower CO₂/N₂ selectivity for the p(SIL) HFMs (Fig. 6).

The CO₂ and N₂ diffusivity and solubility of the p(SIL) HFMs were calculated and are listed in Table 1. When the p(SIL) HFMs were synthesized from SIL monomers with longer alkyl chain lengths, the diffusivity of both CO₂ and N₂ increased. These results indicated that a free volume was formed in the structure of p(SIL) HFMs when the alkyl chain length of the cation was increased.

3.4.2. Effect of ZIF-8 addition

Fig. 7 shows the gas separation performance of the ZIF-8/p(SIL) MMHFMs with 1 wt% ZIF-8. The gas permeance of the ZIF-8/p(SIL) MMHFMs increased with an increase in the number of ZIF-8 particles. However, compared with the CO₂/N₂ selectivity of 1Z-p(1C), those of 1Z-p(2C) and 1Z-p(4C) significantly decreased from 26.7 to 23 to 20.7 and 18.8, respectively. At 1 wt% ZIF-8, the CO₂ permeance of 1Z-p(1C) increased by 33% (from 4.8 to 6.4 GPU). Moreover, the CO₂/N₂ selectivity of 1Z-p(1C) was 30, which was slightly higher than that of p(1C). The difference in performances of 1Z-p(1C), 1Z-p(2C), and 1Z-p(4C) are assumed to be induced by the interactions between ZIF-8 and SIL monomers.

As mentioned in Section 3.4.1, the free volume was induced by SIL monomers with longer alkyl chain lengths. When ZIF-8 was added to the structure of p(1C), it was considered that the ZIF-8 and 1C monomers showed ideal compatibility with each other. This was because the 1C monomers had a shorter alkyl chain length that enhanced the adhesion on the surface of ZIF-8. Further, the π - π interactions between the aromatic rings of the SIL monomers and Hmim of ZIF-8 were conjectured to enhance the adhesion of ZIF-8 and SIL monomers. However, it was easy to form the free volume in the inefficient chain packing and interface of

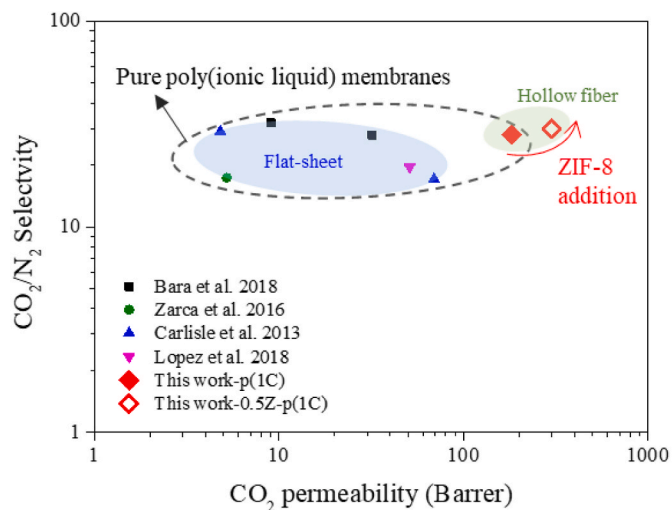
**Fig. 8.** Gas separation performance of ZIF-8/p(SIL) MMHFMs with different alkyl chain lengths.

ZIF-8 and the SIL monomers when the 2C and 4C monomers were used. Therefore, 1Z-p(1C) exhibited higher CO₂ permeance and CO₂/N₂ selectivity than 1Z-p(2C) and 1Z-p(4C).

3.4.3. Optimal loading of ZIF-8

Fig. 8 shows the gas separation performance of the ZIF-8/p(SIL) MMHFMs synthesized by adding 0 to 5 wt% ZIF-8. At 0.5 wt% ZIF-8, the CO₂ permeance of 0.5Z-p(1C) increased by 67% (from 3.6 to 6 GPU). Furthermore, the CO₂/N₂ selectivity of 0.5Z-p(1C) was 30, which was higher than that of p(1C). However, when the loading weight of ZIF-8 was increased from 0.5 to 1 wt% and 5 wt%, the CO₂ permeance of the ZIF-8/p(SIL) MMHFMs decreased from 6 to 4.8 and 4 GPU, respectively. The CO₂/N₂ selectivity of 5Z-p(1C) was slightly decreased at 5 wt% ZIF-8. Therefore, the gas separation performance of ZIF-8/p(SIL) MMHFMs was enhanced at 0.5 wt% ZIF-8, which is beneficial for the separation process. Furthermore, the CO₂ permeance of the ZIF-8/p(SIL) MMHFMs significantly decreased with an increase in the ZIF-8 addition.

The increase in the CO₂ permeance of 0.5Z-p(1C) was because of the

**Fig. 9.** Comparison of the gas separation performance of IL-derived membranes with those of previous studies.

transport pathway provided by the addition of ZIF-8. When 1C monomers were polymerized to form the polymeric chain, the ideal interface interaction with ZIF-8 particles was maintained, and free volume formation was avoided. It is important to avoid the counteraction of the molecular sieve provided by ZIF-8. Therefore, compared to p(1C), the CO₂ permeance of 0.5Z-p(1C) significantly increased without a reduction in the selectivity of CO₂/N₂. Furthermore, the phenomenon of chain rigidification was speculated to cause a lower CO₂ permeance of ZIF-8/p(SIL) MMHFs when the ZIF-8 content was increased from 0.5 to 1 and 5 wt%. The rigidification between the ZIF-8 particles and polymer chains was caused by the reduction in the chain mobility of polymer chains. It was because that the strong adhesion occurs at the interface of the polymer and particles or when the particle addition is increased (Lai et al., 2021; Li et al., 2005; Moore et al., 2004). Therefore, the CO₂ permeance of the ZIF-8/p(SIL) MMHFs was decreased with an increase in ZIF-8 addition from 0.5 to 5 wt%.

3.5. Comparison of the separation performance with previous literature

The gas separation performance of p(1C) and 0.5Z-p(1C) were shown in the Fig. 9 and compared with the pure poly(ionic liquid) membranes reported in previous studies. The configuration of poly(ionic liquid) membranes were flat-sheet which were prepared by coating on the quartz plate (Bara et al., 2008a; Lopez et al., 2018), microporous nylon membrane (Zarca et al., 2016) and porous poly(ether sulfone) (Carlisle et al., 2013). In this study, the poly(ionic liquid) membrane was prepared as the type of hollow fiber. Compared to the flat-sheet, the hollow fiber configuration provided the advantage of large surface area per unit volume. Therefore, p(1C) exhibited higher CO₂ permeability than flat-sheet poly(ionic liquid) membranes reported in previous researches. Additionally, when the ZIF-8 fillers were added into p(1C) to form the ZIF-8/p(SIL) MMHFs, the CO₂ permeability of 0.5Z-p(1C) was increased by 64% from 182 Barrer to 300 Barrer and without CO₂/N₂ selectivity loss. The lower permeability of pure poly(ionic liquid) membranes was a restriction for application due to the dense polymer backbones were synthesized using polymerized IL monomers to form a dense membrane structure (Bara et al., 2008a; Lopez et al., 2018). Therefore, in this study, ZIF-8 nanoparticles, which exhibited the characteristic of the pore size of 3.4 Å and transport pathway, were selected as an ideal filler to beneficially enhance the diffusion of CO₂ gas molecules. However, the phenomenon of chain rigidification was occurred and decreased the CO₂ permeance of membrane when the loading weight of ZIF-8 was increased from 0.5 wt% to 5 wt%. The chain rigidification and filler agglomeration are easily to observe in the structure of MMMs and to decrease the separation performance of MMMs (Dong et al., 2013). Therefore, there is still a challenge need to enhance the addition of filler to improve the separation performance of ZIF-8/p(SIL) MMHFs.

4. Conclusion

In this study, the effects of the alkyl chain length of SIL monomers and the addition of ZIF-8 on the separation performance of ZIF-8/p(SIL) MMHFs were investigated. Before the ZIF-8 addition, p(1C) showed a CO₂/N₂ selectivity of 29, which was higher than that of p(2C) and p(4C). This was because the 1C monomers were composed of short alkyl chain lengths, which avoid inefficient packing in the membrane structure. Compared with p(1C), the CO₂ permeance of 1Z-p(1C) increased from 3.6 to 4.8 GPU without a reduction in CO₂/N₂ selectivity. In addition, the π - π interaction enhanced the compatibility of ZIF-8 and the 1C monomers to form the complete membrane structure of 1Z-p(1C). Furthermore, the 0.5 wt% ZIF-8 was optimal for the preparation of the ZIF-8/p(SIL) MMHFs, which exhibited a CO₂ permeance of 6 GPU and CO₂/N₂ selectivity of 30. This was because a lower amount of ZIF-8 prevented chain rigidification owing to the low chain mobility, which caused a decrease in the CO₂ permeance.

CRedit authorship contribution statement

Wen-Hsiung Lai: Conceptualization, Methodology, Investigation, Data curation, Writing – original draft, Writing – review & editing. **David K. Wang:** Conceptualization, Methodology. **Ming-Yen Wey:** Conceptualization, Methodology, Writing – review & editing, Supervision, Project administration, Funding acquisition. **Hui-Hsin Tseng:** Conceptualization, Methodology, Writing – review & editing, Supervision.

Declaration of competing interest

The authors declare that they have no known competing financial interests or personal relationships that could have appeared to influence the work reported in this paper.

Data availability

Data will be made available on request.

Acknowledgements

The authors greatly appreciate financial support from the Ministry of Science and Technology (MOST-107-2221-E-005-004-MY3).

Appendix A. Supplementary data

Supplementary data to this article can be found online at <https://doi.org/10.1016/j.jclepro.2022.133785>.

References

- Albo, J., Wang, J., Tsuru, T., 2014. Gas transport properties of interfacially polymerized polyamide composite membranes under different pre-treatments and temperatures. *J. Membr. Sci.* 449, 109–118.
- Aroon, M.A., Ismail, A.F., Matsuura, T., Montazer-Rahmati, M.M., 2010. Performance studies of mixed matrix membranes for gas separation: a review. *Separ. Purif. Technol.* 75 (3), 229–242.
- Bara, J.E., Gabriel, C.J., Hatakeyama, E.S., Carlisle, T.K., Lessmann, S., Noble, R.D., Gin, D.L., 2008a. Improving CO₂ selectivity in polymerized room-temperature ionic liquid gas separation membranes through incorporation of polar substituents. *J. Membr. Sci.* 321 (1), 3–7.
- Bara, J.E., Hatakeyama, E.S., Gin, D.L., Noble, R.D., 2008b. Improving CO₂ permeability in polymerized room-temperature ionic liquid gas separation membranes through the formation of a solid composite with a room-temperature ionic liquid. *Polym. Adv. Technol.* 19 (10), 1415–1420.
- Bara, J.E., Lessmann, S., Gabriel, C.J., Hatakeyama, E.S., Noble, R.D., Gin, D.L., 2007. Synthesis and performance of polymerizable room-temperature ionic liquids as gas separation membranes. *Ind. Eng. Chem. Res.* 46 (16), 5397–5404.
- Bara, J.E., Noble, R.D., Gin, D.L., 2009. Effect of “free” cation substituent on gas separation performance of Polymer–Room-temperature ionic liquid composite membranes. *Ind. Eng. Chem. Res.* 48 (9), 4607–4610.
- Basu, S., Cano-Odena, A., Vankelecom, I.F.J., 2011. MOF-containing mixed-matrix membranes for CO₂/CH₄ and CO₂/N₂ binary gas mixture separations. *Separ. Purif. Technol.* 81 (1), 31–40.
- Carlisle, T.K., Wiesenauer, E.F., Nicodemus, G.D., Gin, D.L., Noble, R.D., 2013. Ideal CO₂/light gas separation performance of poly(vinylimidazolium) membranes and poly(vinylimidazolium)-ionic liquid composite films. *Ind. Eng. Chem. Res.* 52 (3), 1023–1032.
- Ceratti, D.R., Faustini, M., Sinturel, C., Vayer, M., Dahirel, V., Jardat, M., Grosso, D., 2015. Critical effect of pore characteristics on capillary infiltration in mesoporous films. *Nanoscale* 7 (12), 5371–5382.
- Chen, B., Bai, F., Zhu, Y., Xia, Y., 2014a. A cost-effective method for the synthesis of zeolitic imidazolate framework-8 materials from stoichiometric precursors via aqueous ammonia modulation at room temperature. *Microporous Mesoporous Mater.* 193, 7–14.
- Chen, B., Bai, F., Zhu, Y., Xia, Y., 2014b. Hofmeister anion effect on the formation of ZIF-8 with tuneable morphologies and textural properties from stoichiometric precursors in aqueous ammonia solution. *RSC Adv.* 4 (88), 47421–47428.
- Chen, X., Zhou, M., Hou, Q., Tu, X., Wu, X., 2013. Active poly(4-chloromethyl styrene)-functionalized multiwalled carbon nanotubes. *Macromol. Chem. Phys.* 214 (16), 1829–1835.
- Chung, T.-S., Hu, X., 1997. Effect of air-gap distance on the morphology and thermal properties of polyethersulfone hollow fibers. *J. Appl. Polym. Sci.* 66 (6), 1067–1077.
- Cowan, M.G., Masuda, M., McDanel, W.M., Kohno, Y., Gin, D.L., Noble, R.D., 2016. Phosphonium-based poly(Ionic liquid) membranes: the effect of cation alkyl chain

- length on light gas separation properties and ionic conductivity. *J. Membr. Sci.* 498, 408–413.
- Cravillon, J., Nayuk, R., Springer, S., Feldhoff, A., Huber, K., Wiebcke, M., 2011. Controlling zeolitic imidazolate framework nano- and microcrystal formation: insight into crystal growth by time-resolved in situ static light scattering. *Chem. Mater.* 23 (8), 2130–2141.
- Dai, Y., Johnson, J.R., Karvan, O., Sholl, D.S., Koros, W.J., 2012. Ultem®/ZIF-8 mixed matrix hollow fiber membranes for CO₂/N₂ separations. *J. Membr. Sci.* 401–402, 76–82.
- Dong, G., Li, H., Chen, V., 2013. Challenges and opportunities for mixed-matrix membranes for gas separation. *J. Mater. Chem. A* 1 (15), 4610–4630.
- Friess, K., Izák, P., Kárászová, M., Pasichnyk, M., Lanč, M., Nikolaeva, D., Luis, P., Jansen, J.C., 2021. A review on ionic liquid gas separation membranes. *Membranes* 11 (2), 97.
- Ghasemi Estahbanati, E., Omidkhan, M., Ebadi Amooghini, A., 2017. Preparation and characterization of novel ionic liquid/Pebax membranes for efficient CO₂/light gases separation. *J. Ind. Eng. Chem.* 51, 77–89.
- Guan, W., Dai, Y., Dong, C., Yang, X., Xi, Y., 2020. Zeolite imidazolate framework (ZIF)-based mixed matrix membranes for CO₂ separation: a review. *J. Appl. Polym. Sci.* 137 (33), 48968.
- He, M., Yao, J., Liu, Q., Wang, K., Chen, F., Wang, H., 2014. Facile synthesis of zeolitic imidazolate framework-8 from a concentrated aqueous solution. *Microporous Mesoporous Mater.* 184, 55–60.
- Hosseini, S.S., Peng, N., Chung, T.S., 2010. Gas separation membranes developed through integration of polymer blending and dual-layer hollow fiber spinning process for hydrogen and natural gas enrichments. *J. Membr. Sci.* 349 (1), 156–166.
- Huang, T.-C., Liu, Y.-C., Lin, G.-S., Lin, C.-H., Liu, W.-R., Tung, K.-L., 2020. Fabrication of pebax-1657-based mixed-matrix membranes incorporating N-doped few-layer graphene for carbon dioxide capture enhancement. *J. Membr. Sci.* 602, 117946.
- Ismail, A.F., Goh, P.S., Sanip, S.M., Aziz, M., 2009. Transport and separation properties of carbon nanotube-mixed matrix membrane. *Separ. Purif. Technol.* 70 (1), 12–26.
- Jian, M., Liu, B., Liu, R., Qu, J., Wang, H., Zhang, X., 2015. Water-based synthesis of zeolitic imidazolate framework-8 with high morphology level at room temperature. *RSC Adv.* 5 (60), 48433–48441.
- Kammakakam, I., Bara, J.E., Jackson, E.M., 2020. Dual anion-cation crosslinked poly(ionic liquid) composite membranes for enhanced CO₂ separation. *ACS Appl. Polym. Mater.* 2 (11), 5067–5076.
- Kida, K., Okita, M., Fujita, K., Tanaka, S., Miyake, Y., 2013. Formation of high crystalline ZIF-8 in an aqueous solution. *Crystrngcomm* 15 (9), 1794–1801.
- Kimura, E., Kurogi, Y., Takahashi, T., 1991. The first gold (III) macrocyclic polyamine complexes and application to selective gold (III) uptake. *Inorg. Chem.* 30 (22), 4117–4121.
- Lai, W.-H., Wang, D.K., Tseng, H.-H., Wey, M.-Y., 2022. Photo-induced poly(styrene-[C₁mim][Tf₂N])-supported hollow fiber ionic liquid membranes to enhance CO₂ separation. *J. CO₂ Util.* 56, 101871.
- Lai, W.-H., Wang, D.K., Wey, M.-Y., Tseng, H.-H., 2020. Recycling waste plastics as hollow fiber substrates to improve the anti-wettability of supported ionic liquid membranes for CO₂ separation. *J. Clean. Prod.* 276, 124194.
- Lai, W.-H., Wey, M.-Y., Tseng, H.-H., 2021. High loading and high-selectivity H₂ purification using SBC@ZIF based thin film composite hollow fiber membranes. *J. Membr. Sci.* 626, 119191.
- Lai, W.-H., Zhuang, G.-L., Tseng, H.-H., Wey, M.-Y., 2019. Creation of tiny defects in ZIF-8 by thermal annealing to improve the CO₂/N₂ separation of mixed matrix membranes. *J. Membr. Sci.* 572, 410–418.
- Li, B., Zhao, S., Zhu, J., Ge, S., Xing, K., Sokolov, A.P., Saito, T., Cao, P.-F., 2021. Rational polymer design of stretchable poly(ionic liquid) membranes for dual applications. *Macromolecules* 54 (2), 896–905.
- Li, Y., Chung, T.-S., Cao, C., Kulprathipanja, S., 2005. The effects of polymer chain rigidification, zeolite pore size and pore blockage on polyethersulfone (PES)-zeolite A mixed matrix membranes. *J. Membr. Sci.* 260 (1), 45–55.
- Liang, L., Gan, Q., Nancarrow, P., 2014. Composite ionic liquid and polymer membranes for gas separation at elevated temperatures. *J. Membr. Sci.* 450, 407–417.
- Lin, G.-S., Chen, Y.-R., Chang, T.-H., Huang, T.-C., Zhuang, G.-L., Huang, W.-Z., Liu, Y.-C., Matsuyama, H., Wu, K.C.W., Tung, K.-L., 2021. A high ZIF-8 loading PVA mixed matrix membrane on alumina hollow fiber with enhanced ethanol dehydration. *J. Membr. Sci.* 621, 118935.
- Lin, Y.-C., Liu, K.-M., Chiu, P.-L., Chao, C.-M., Wen, C.-S., Wang, C.-Y., Tseng, H.-H., 2022. Enhancing the hydrophilicity and biofoulant removal ability of a PVDF ultrafiltration membrane via π - π interactions as measured by AFM. *J. Membr. Sci.* 641, 119874.
- Lin, Y.-T., Wey, M.-Y., Tseng, H.-H., 2021. Highly permeable mixed matrix hollow fiber membrane as a latent route for hydrogen purification from hydrocarbons/carbon dioxide. *Membranes* 11 (11), 865.
- Lopez, A.M., Cowan, M.G., Gin, D.L., Noble, R.D., 2018. Phosphonium-Based poly(ionic liquid)/ionic liquid ion gel membranes: influence of structure and ionic liquid loading on ion conductivity and light gas separation performance. *J. Chem. Eng. Data* 63 (5), 1154–1162.
- Ma, C., Zhang, C., Labreche, Y., Fu, S., Liu, L., Koros, W.J., 2015. Thin-skinned intrinsically defect-free asymmetric mono-esterified hollow fiber precursors for crosslinkable polyimide gas separation membranes. *J. Membr. Sci.* 493, 252–262.
- Moore, T.T., Mahajan, R., Vu, D.Q., Koros, W.J., 2004. Hybrid membrane materials comprising organic polymers with rigid dispersed phases. *AIChE J.* 50 (2), 311–321.
- Neves, L.A., Crespo, J.G., Coelho, I.M., 2010. Gas permeation studies in supported ionic liquid membranes. *J. Membr. Sci.* 357 (1), 160–170.
- Nik, O.G., Chen, X.Y., Kaliaguine, S., 2012. Functionalized metal organic framework-polyimide mixed matrix membranes for CO₂/CH₄ separation. *J. Membr. Sci.* 413–414, 48–61.
- Nordin, N.A.H.M., Ismail, A.F., Mustafa, A., Murali, R.S., Matsuura, T., 2014. The impact of ZIF-8 particle size and heat treatment on CO₂/CH₄ separation using asymmetric mixed matrix membrane. *RSC Adv.* 4 (94), 52530–52541.
- Ordoñez, M.J.C., Balkus, K.J., Ferraris, J.P., Musselman, I.H., 2010. Molecular sieving realized with ZIF-8/Matrimid® mixed-matrix membranes. *J. Membr. Sci.* 361 (1), 28–37.
- Peng, N., Chung, T.S., 2008. The effects of spinneret dimension and hollow fiber diameter on gas separation performance of ultra-thin defect-free Torlon® hollow fiber membranes. *J. Membr. Sci.* 310 (1), 455–465.
- Perez, E.V., Balkus, K.J., Ferraris, J.P., Musselman, I.H., 2009. Mixed-matrix membranes containing MOF-5 for gas separations. *J. Membr. Sci.* 328 (1), 165–173.
- Ríos, A.P.d.l., Hernández-Fernández, F.J., Tomás-Alonso, F., Palacios, J.M., Gómez, D., Rubio, M., Villora, G., 2007. A SEM-EDX study of highly stable supported liquid membranes based on ionic liquids. *J. Membr. Sci.* 300 (1), 88–94.
- Sasikumar, B., Arthanareeswaran, G., Ismail, A.F., 2018. Recent progress in ionic liquid membranes for gas separation. *J. Mol. Liq.* 266, 330–341.
- Shamair, Z., Habib, N., Gilani, M.A., Khan, A.L., 2020. Theoretical and experimental investigation of CO₂ separation from CH₄ and N₂ through supported ionic liquid membranes. *Appl. Energy* 268, 115016.
- Tang, J., Radosz, M., Shen, Y., 2008. Poly(ionic liquid)s as optically transparent microwave-absorbing materials. *Macromolecules* 41 (2), 493–496.
- Tomé, L.C., Florindo, C., Freire, C.S.R., Rebelo, L.P.N., Marrucho, I.M., 2014. Playing with ionic liquid mixtures to design engineered CO₂ separation membranes. *Phys. Chem. Chem. Phys.* 16 (32), 17172–17182.
- Tomé, L.C., Marrucho, I.M., 2016. Ionic liquid-based materials: a platform to design engineered CO₂ separation membranes. *Chem. Soc. Rev.* 45 (10), 2785–2824.
- Wang, Q., Sun, Y., Li, S., Zhang, P., Yao, Q., 2020. Synthesis and modification of ZIF-8 and its application in drug delivery and tumor therapy. *RSC Adv.* 10 (62), 37600–37620.
- Wang, X., Zhuo, N., Fu, C., Tian, Z., Li, H., Zhang, J., Wu, W., Yang, Z., Yang, W., 2017. Enhanced selective adsorption of benzotriazole onto nanosized zeolitic imidazolate frameworks confined in polystyrene anion exchanger. *Chem. Eng. J.* 328, 816–824.
- Wijayanayake, S.N., Panapitiya, N.P., Nguyen, C.N., Huang, Y., Balkus, K.J., Musselman, I. H., Ferraris, J.P., 2014. Composite membranes with a highly selective polymer skin for hydrogen separation. *Separ. Purif. Technol.* 135, 190–198.
- Wijayanayake, S.N., Panapitiya, N.P., Versteeg, S.H., Nguyen, C.N., Goel, S., Balkus, K.J., Musselman, I.H., Ferraris, J.P., 2013. Surface cross-linking of ZIF-8/polyimide mixed matrix membranes (MMMs) for gas separation. *Ind. Eng. Chem. Res.* 52 (21), 6991–7001.
- Yuan, X., Yu, H., Xu, S., Huo, G., Cornelius, C.J., Fan, Y., Li, N., 2022. Performance optimization of imidazole containing copolyimide/functionalized ZIF-8 mixed matrix membrane for gas separations. *J. Membr. Sci.* 644, 120071.
- Zarca, G., Horne, W.J., Ortiz, I., Urriaga, A., Bara, J.E., 2016. Synthesis and gas separation properties of poly(ionic liquid)-ionic liquid composite membranes containing a copper salt. *J. Membr. Sci.* 515, 109–114.
- Zhuang, G.-L., Tseng, H.-H., Uchytel, P., Wey, M.-Y., 2018. Enhancing the CO₂ plasticization resistance of PS mixed-matrix membrane by blunt zeolitic imidazolate framework. *J. CO₂ Util.* 25, 79–88.